Ionic Adsorption of Lithium Bromide at the Mercury-Dimethyl Sulfoxide Interface

Kohichi YAMAMOTO and Shigeo HAYANO
Institute of Industrial Science, University of Tokyo, Minato-ku, Tokyo 106
(Received June 23, 1975)

The specific adsorption of bromide ions on a mercury electrode from lithium bromide solutions of dimethyl sulfoxide (DMSO) has been studied through the measurement of the differential capacity and the interfacial tension. The capacity data showed the evidence that anions are more weakly, but cations are more strongly, solvated by DMSO molecules than by H_2O. The amounts of specifically adsorbed bromide ions are greater than those values in water at the same electrode charge. The specific adsorption of cations (Li^+) was not found in this study. The inner layer capacity due to the amounts of specific adsorbed anions was calculated, and the ratio of the distances from the metal to the inner Helmholtz plane and to the outer Helmholtz plane were deduced. These values are comparable to those for LiCl in DMSO, but are greater than for water.

Many works on the specific adsorption and the inner layer structure of the electrical double layer have been reported in aqueous system. However, these have been few on non-aqueous systems, especially aprotic solvent systems. It is well known that the role of solvent molecules is very important in the structure of the electrical double layer. An aprotic solvent like dimethyl sulfoxide (DMSO) is very favourable for investigating the electrical double layer, for we can exclude the contribution due to protons. On the other hand, DMSO has been the subject of many recent electrochemical studies[1-4] directed towards the design of new battery systems. The specific adsorption of the supporting electrolyte on the electrode surface has a great influence on these studies. Furthermore, it will be necessary, for a detailed description of electrode kinetics, to analyze the structure of the electrical double layer.

Kolthoff and Reddy[5] obtained an electrocapillary curve of the 0.1M NaCl solution in DMSO. Payne[6] measured the electrocapillary curves and differencial capacities of the double layer for various inorganic salts in DMSO and in mixtures of DMSO and water. However, these studies did not attempt to go into any quantitative discussion of adsorbed ions because of the lack of thermodynamic data. Kim *et al.*[7] discussed the structure of the electrical dorble layer in the presence of LiCl from the measurement of the electrocapillary curves. Hills and Reeves[8] measured the activity coefficients of $LiNO_3$ in DMSO and investigated the degree of ionic adsorption from the measurement of the differential capacities. These two recent detailed studies, however, are different from each other in several points (*e.g.* regarding the solvent effect) in spite of the similar method of data analysis. It is important to investigate systematically halide ions (*e.g.* LiCl, LiB, LiI) in DMSO for the purpose of describing the structure of the electrical double layer and the ionic adsorption in detail. Therefore, a comparison of the above data with the corresponding data for aqueous systems will be useful in discussing the role of solvent molecules.

In the present paper, we will attempt to examine the structure of the electrical double layer in mercury–DMSO containing LiBr. The thermodynamic parameters for the double layer were calculated through measurements of the differential capacity and the interfacial tension.

Experimental

Differential capacity-potential curves were obtained by measuring the in- and out of-phase components of the AC admittance of the mercury electrode–DMSO solution interface by the use of a PAR model 170 electrochemistry system. A 10 mV (peak to peak) amplitude AC voltage with a frequency of 80 Hz was superimposed on the DC voltage applied between the dropping mercuy electrode (DME) and the platinum counter electrode. The scan rate of the DC voltage was 1 mV/s. The drop time of mercury was mechanically controlled at 5 s, and the capillary constant, m, for DME was 0.739 mg/s. The amplitudes of the in- and out of-phase components were recorded as a function of the DME potential. The differential capacity, C, was calculated from:

$$C = \frac{I_i^2 + I_0^2}{2\pi f I_0 V A} \quad (1)$$

where I_i is the AC current of the in-phase, I_0 is that of the out of-phas,e f is the frequency (Hz), V is its amplitude, and A is the area of the electrode at the end of the drop life, as calculated from the flow rate and the drop time. The precision of the data obtained in this manner was about 0.5%.

The interfacial tension between the mercury electrode and the DMSO solution was measured at the electrocapillary maximum (*i.e.*, point of zero charge) to determine the integral constant in the process of the integration of the capacity-potential curve. This has been done by using a modified Lippmann type capillary electrometer. The capillary electrometer used in this work was constructed by taking several ideas presented by previous workers.[9-11] The tapering capillary was made of a Pyrex capillary tubing with an internal diameter of 1 mm. The tubing was drawn out in a gas flame so as to have the internal diameter of 15—20 μ. Then the capillary was cut at this point. The gas pressure above the mercury reservoir was controlled by a nitrogen gas pressure control system which consists of a series combination of two precision-variable bellows mounted over a screwdriven press. The gas pressure was measured with a Texas Instruments, Inc. Fused-Quartz Precision Pressure Gauge instead of a mercury manometer. A stereomicroscope was employed to observe the capillary tip. The window of the cell was finished to an optically plane to eliminate distortion. The precision of the interfacial tension in this methods is within 0.02%. For the measurements of both the differential capacity and the interfacial tension, the temperature of the cell was controlled at 25.0±0.1 °C. Prior to each measurement the solution was flushed with a high-purity nitrogen which had been deoxygenated, dehydrated in an anhydrous

calcium chloride column, and then presaturated by bubbling it through DMSO. DMSO was refluxed for several hours on calcium hydride and then fractionated through an efficient distillation column at a reduced pressure of about 5 Torr. The water content of the solvent was checked by means of Karl Fisher titration. The analytical reagent grade mercury was used without further purification, while the analytical grade anhydrous LiBr was used after have been dried at 180 °C under a vacuum for 24 hr.

Results and Discussion

Differential capacity *vs.* potential curves for LiBr in DMSO at six concentration levels between 0.753 M and 0.0196 M were obtained in the potential range of −0.35∼−1.65 V (*vs.* aqueous SCE), where no significant DC current and no frequency dispersion of capacity was observed. At more positive potentials, the measurements were not reproducible, this is due to the faradaic admittance. The aqueous SCE was used as a reference electrode, the junction between the reference electrode and the DMSO solution was kept constant in each experiment by employing the 0.200 M LiBr solution in DMSO. The liquid junction between 0.200 M solution and the test solution was made through a fritted glass. The measured potentials, E_m, were converted to the potential scale of the reference electrode reversible to the anion (*i.e.*, to the E^- scale) according to this equation:

$$E^- = E_m + E_{ljp} + \frac{RT}{F} \ln a_{\pm} \quad (2)$$

Here, E_{ljp} is the liquid junction potential between 0.200 M and x M LiBr in DMSO (test solution); it was calculated using the following equation:

$$E_{ljp} = (2t^+ - 1)\frac{RT}{F} \ln \frac{a_{\pm}}{a_{\pm 0.200M}} \quad (3)$$

The mean ionic activities, $a_{\pm}$, were taken form the data of Salomon.[12] The transference number for Li^+ in DMSO, t^+, was estimated to be 0.324 from the mobility data of Dunnett and Gasser.[13] The observed differential capacity *vs.* potential (converted to E^- scale) curves are shown in Fig. 1. The curves are featureless like those of the LiCl[7] and $LiNO_3$[8] solutions in DMSO. The capacity increases rapidly in the anodic branch; this is due to the specific adsorption of the anion. The anodic hump in the capacity curves observed in the cases of $LiClO_4$[6] and KPF_6[6,14] in DMSO were not found anywhere in the concentration range studied. The diffuse layer capacity minimum, which was observed with KPF_6,[6] $LiNO_3$,[8] KNO_3[14] in DMSO, was not detected even in the 0.0196 M LiBr solution. The diffuse layer capacity minimum appears in the vicinity of pzc if there is no significant ionic specific adsorption; *i.e.*, the structure of the double layer can be assumed to be a simple Stern model. Therefore, the differential capacity curves shown in Fig. 1 lead us to the conclusion that Br^- is more specifically adsorbed on the mercury electrode than PF_6^-, ClO_4^- and NO_3^-. In the cathodic branch, the capacity decreases monotonously with the electrode potential to the value of about 7 μF/cm². This limiting value is comparable with that obtained in DMSO containing lithium salt.[6-8] In aqueous systems, in general, at higher cathodic potentials a rise in the capacity curves is observed. This is due to the onset of the faradaic reaction. In the present system, such behaviour was not detectable, so, in the potential region of the invariant capacity (*i.e.*, at extreme cathodic potentials), the structure of the electrical double layer may be determined mainly by the Li^+ cation, which is more firmly solvated in DMSO than in aqueous solutions. This point will be discussed later in detail. The difference in the limiting value in DMSO from those in aqueous solutions (about 16 μF/cm²) can be expected from the lower dielectric constant of DMSO, since, in these potential regions, we can assume that there is no ionic specific adsorption.

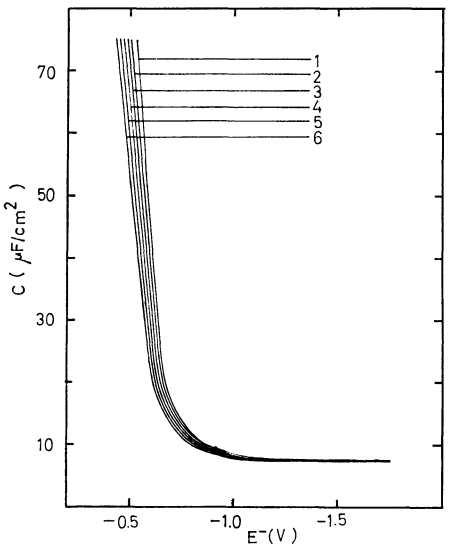

Fig. 1. Differential capacity of electrical double layer at mercury electrode in contact with LiBr solutions in DMSO at 25 °C: (1): 0.753 M, (2): 0.497 M, (3): 0.196 M, (4): 0.0979 M, (5): 0.0497 M, (6): 0.0196 M.

For a detailed discussion, it is a matter of prime importance to establish to what degree bromide ions are specifically adsorbed from DMSO. The capacity *vs.* potential data were integrated to obtain the charge density on the electrode, q_m, and the interfacial tension, γ, over the entire range of concentrations and potentials with the aid of a computer (FACOM 230-55) using a program written in FORTRAN. Then Parsons' auxiliary function, ξ,[15] was evaluated from this equation:

$$\xi_- = \gamma + q_m E^- \quad (4)$$

The surface excess of Li^+ cations, Γ_+, was then calculated from this relationship:

$$\left(\frac{\partial \xi_-}{2RT\partial \ln a_{\pm}}\right)_{q_m} = -\Gamma_+ = -\frac{q_+}{F} \quad (5)$$

This calculation was carried out first by computer differentiation and then checked manually. The results, expressed as q_+ (*i.e.*, the charge due to the excess of cations), are shown in Fig. 2. This shows that the bromide ion is adsorbed so strongly that the surface excess of lithium ions is positive at all concentrations and all values of q_m. Figure 2 also shows a minimum at all concentrations which is similar to those found with

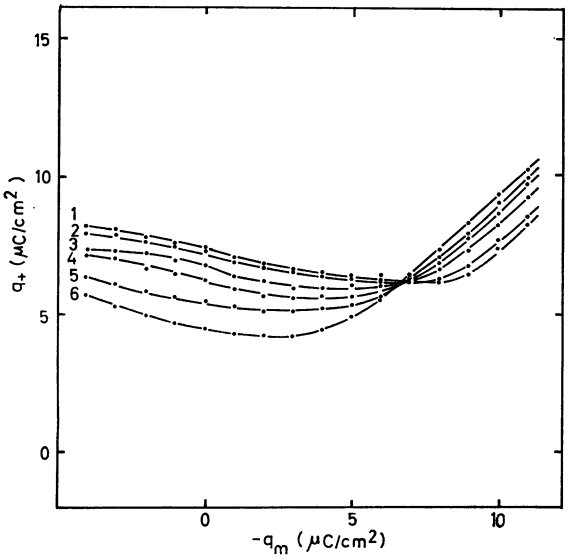

Fig. 2. Charge due to the cations as a function of the electrode charge (q_m) at the corresponding concentration as given in Fig. 1.

LiCl[7] and $LiNO_3$[8] in DMSO and with aqueous solutions of strongly adsorbed species, such as halide ions.[16] The appearence of the invariant point at $q_m = -7$ μC/cm^2 is interesting; such a point is also found in the comparable study of LiCl in DMSO.[7] This invariant point, however, is more negative than those of chloride ions ($q_m = -4$ μC/cm^2).

From the similarity of the surface excess curve with those for aqueous alkali halide solutions[16-17] and the results obtained in the present work, it seems reasonable to assume that lithium ions are present only in the diffuse layer. That is, $q_+ = q_+^{2-s}$, where q_+^{2-s} is the charge in the diffuse layer. On the basis of this assumption, we calculated the potential of the outer Helmholtz plane, ϕ_2, from q_+^{2-s} according to the diffuse layer theory;[18]

$$q_+^{2-s} = \left(\frac{RT\varepsilon C^s}{2\pi}\right)^{1/2}\left[\exp\left(-\frac{F}{2RT}\phi_2\right)-1\right] \qquad (6)$$

Here, C^s is the electrolyte concentration and ε is the dielectric constant in the diffuse layer, assuming it to be equal to the bulk dielectric constant of DMSO (46.7).[19] Then the charge due to the bromide ions, q_-, and that distributed in the diffuse (q_-^{2-s}) and inner (q_-) fouble layer were evaluated according to:

$$-q_m = q_+^{2-s} + q_- \qquad (7)$$

$$q_- = q_-^{2-s} + q_-^1 \qquad (8)$$

$$q_-^{2-s} = -\left(\frac{RT\varepsilon C^s}{2\pi}\right)^{1/2}\left[\exp\left(\frac{F}{2RT}\phi_2\right)-1\right] \qquad (9)$$

The plots of ϕ_2 *vs.* q_m as a function of the LiBr concentration are shown in Fig. 3. The curves have a striking resemblance to those of the LiCl solution.[7] In the absence of a specific adsorption such as in NaF aqueous solutions,[20-21] the sign of ϕ_2 changes at pzc. However, in the present system, the specific adsorption of bromide ions is so strong that ϕ_2 is negative over the entire range of q_m and the values of ϕ_2 are more negative than those obtained in chloride ions.

The specifically adsorbed charge due to bromide ions

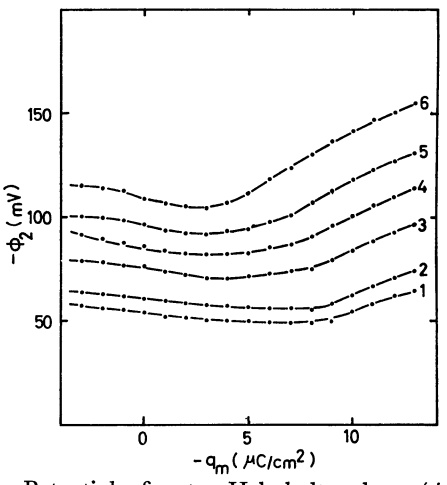

Fig. 3. Potential of outer Helmholtz plane (ϕ_2) as a function of the value of q_m at various LiBr concentrations.

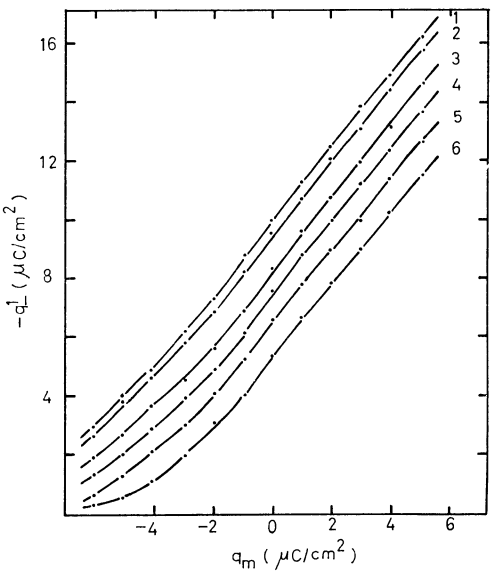

Fig. 4. Charge due to specifically adsorbed bromide ions (q_-^1) as a function of the electrode charge at the corresponding concentration as given in Fig. 1.

(q_-^1) is shown in Fig. 4 as a function of q_m and the LiBr concentration. The figure shows that q_-^1 is a monotonous function of q_m and that the degree of the concentration dependence of q_-^1 changes with q_m, that is, increases with the electrode charge. This behaviour is similar to that found in chloride ions[7] in DMSO and is different from that in nitrate ions[8] in DMSO (*i.e.*, the nitrate-ions system shows a reversed tendency.). At $q_m > 0$ the curves become virtually parallel lines. At the same concentration, say at 0.1 M, some comparisons can be made with the system of other electrolytes in DMSO and with the aqueous potassium bromide solution. The minimum q_m value (0 μC/cm^2), the $q_-^1 - q_m$ curves of which in Fig. 4 deviate from a straight line, is more negative than those obtained in chloride ions[7] and nitrate ions[8] in DMSO (*ca.* 2 and 4 μC/cm^2 respectively), but it is more positive than that with potassium iodide in formamide[22] (*ca.* -2 μC/cm^2). The values of the specifically adsorbed charge at pzc are as

follows; −7.5 (in the present system), −5.1 (in KBr aqueous solution),[17] −4.5 (in LiCl solution in DMSO),[7] −3.6 (in $LiNO_3$ solution in DMSO)[8] and −1.2 (in KPF_6 solution in DMSO)[14] (unit is $\mu C/cm^2$). From these results, it may be concluded that the degree of the specific adsorption of anions in DMSO changes in the following order:

$$PF_6^- < NO_3^- < Cl^- < Br^-$$

and the specific adsorption of bromide ions is stronger in DMSO than in H_2O.

The limiting values of the slope at positive q_m values were −1.26~−1.35. These values of the dq_-^1/dq_m will be discussed in the section on Esin and Markov effects below.

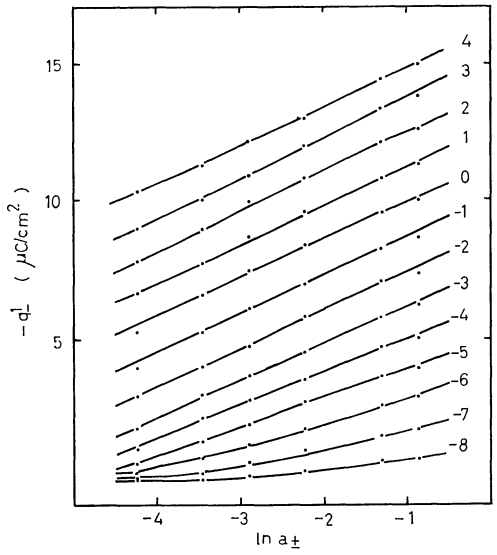

Fig. 5. Charge due to specifically adsorbed bromide ions (q_-^1) as a function of ln $a_\pm$ at the constant value of charge on electrode (q_m). The value of q_m is indicated by each line in $\mu C/cm^2$.

We also show the logarithmic isotherms at a constant q_m in Fig. 5. The figure is similar in character to that obtained for aqueous bromide and iodide solutions.

It is usual to invenstigate the degree of specific adsorption in terms of the Esin and Markov coefficients, defined as:[23-24]

$$\left(\frac{\partial E^+}{\partial \mu}\right)_{q_m} = -\left(\frac{\partial \Gamma_-}{\partial q_m}\right)_\mu \tag{10}$$

or

$$\left(\frac{\partial E^+}{\partial \ln a_\pm}\right)_{q_m} = \frac{2RT}{F}\left[\left(\frac{\partial q_-^1}{\partial q_m}\right)_\mu + \left(\frac{\partial q_-^{2-s}}{\partial q_m}\right)_\mu\right] \tag{11}$$

where E^+ is the potential with respect to the reference electrode reversible to the cation. The right-hand sides of Eq. (10) and (11) can be predicted as follows from the diffiuse double layer theory in the absence of any specific adsorption:

$$\left(\frac{\partial E^+}{\partial \ln a_\pm}\right)_{q_m} = -\frac{1}{2}\exp\left[\sinh^{-1}\left(\frac{q_m}{2A}\right)\right]\left[1+\left(\frac{q_m}{2A}\right)^2\right]^{-1/2}$$

$$A = \left(\frac{RT\varepsilon C^s}{2\pi}\right)^{1/2} \tag{12}$$

The observed results are shown in Fig. 6. According to Eq. (12), if any specific adsorption is absent, two

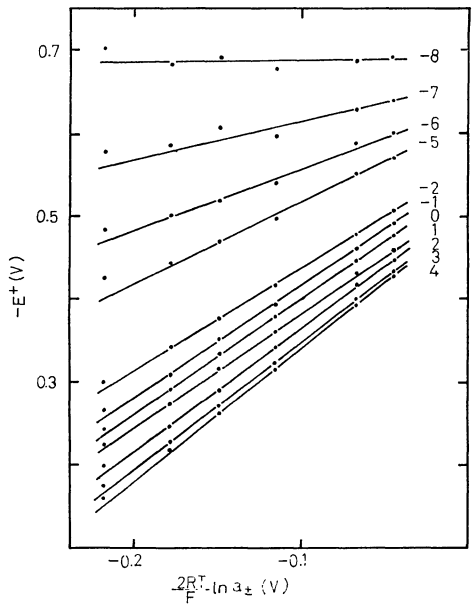

Fig. 6. Esin and Markov plots for LiBr in DMSO at 25 °C. The value of q_m in $\mu C/cm^2$ is incicated by each line.

limiting slopes can be found, *i.e.*, 0 for $q_m \to -\infty$ and −1 for $q_m \to +\infty$ respectively. Furthermore, the value of the slope is −0.5 at pzc (*i.e.*, at $q_m=0$). In this study, however, the values of the slope evidently deviate from those given by Eq. (12); that is because of the significant specific adsorption of bromide ions. The slope becomes steeper with an increase in the electrode charge. At pzc this value is −1.2, and it reaches the limiting value of −1.3 at $q_m=4\ \mu C/cm^2$. This limiting value is compared with those obtained for other electrolytes in DMSO in Table 1. In the second row, the values of $-(\partial q_-^1/\partial q_m)_\mu$ (*i.e.*, the derivatives of the adsorbed anion charge with respect to the electrode charge at a constant chemical potential) are shown. It is well known that the Esin and Markov coefficients are approximately equal to this value[7-8,25] (*cf.* Eq. (11)). In the present work, the two values agree well. This shows the consistency of the experimental data. The values for LiBr in the first row and in the second row in Table 1 are the highest among the electrolytes. The high specific adsorptivity of the bromide ions was confirmed again by these results.

In the discussion of the specific adsorption of ions, we must take into account two important factors. One is the solvation energy of ions, and the other is the interaction between the metal surface and solvent molecules. According to Parker,[26] such dipolar aprotic

Table 1. The limiting values of Esin and Markov coefficient for various anions in DMSO

	LiBr	LiCl	$LiNO_3$	KPF_6
$-\frac{F}{2RT}\left(\frac{\partial E^+}{\partial \ln a_\pm}\right)_{q_m}$	1.3	1.2	1.18	1.26
$-\left(\frac{\partial q_-^1}{\partial q_m}\right)_\mu$	1.26—1.35	1.1—1.3	1.17[a]	1.26[a]
Reference		7)	8)	25)

a) The value was taken for 0.1 M solution.

solvents as DMSO poorly solvate anion.[12,27] Salomon has reported that the free energy of transfer of LiBr from H_2O to DMSO at 25 °C is 2.515 kcal/mol, and concluded that the order of increasing solvation by DMSO molecules is:

$$Cl^- < Br^- < I^-$$

in spite of the solvation being poorer than the H_2O system. This behaviour is reflected in our study by the rapid rise on the capacity curves in the anodic potential in Fig. 1. Furthermore, as for the ionic solvation, we may infer that the small cations like Li^+ are solvated more steadily in DMSO than in H_2O. This is supported by the evidence that the significant capacity rise found in the case of an aqueous system was not observed in Fig. 1. From these results, the higher specific adsorptivity of bromide ions in the DMSO system seems to be attributable to the difference in the degree of ionic solvation. However, the second factor (*i.e.*, the interction of the mercury electrode surface and the DMSO molecules) is also important, as was pointed out by Hills *et al.*[8] The effect of this factor can be observed on the values of the Esin and Markov coefficients and $-(\partial q_-^1/\partial q_m)_\mu$. These values in Table 1 are higher than those of aqueous solutions for other electrolytes. This may be the influence of the property of the solvent molecules. Hills *et al.*[8] stressed this factor in their study of $LiNO_3$ in DMSO, since the value of $-(\partial q_-^1/\partial q_m)_\mu$ rises with the electrode charge. These values are higher in their system than in the corresponding aqueous system (up to 1.3 for DMSO and 1.22 for water). In our present work, however, we did not observed such a significant difference between these two systems. It is difficult and dangerous to conclude which factor predominantly governs the specific adsorption of ions from only these data. Independent measurements from this point of view are desirable.

For the detailed discussion of the structure of the inner layer, the potential drop across the layer between the electrode surface and the outer Helmholtz plane (oHp), $\phi_{m-2'}$ was calculated from this relationship:[7,22]

$$\phi_{m-2} = E_m + E_{ljp} - \phi_2 \tag{13}$$

Here, it should be mentioned that the ϕ_{m-2} potential computed in this way is not equal to the rational potential in the sense of Grahame's definition. ϕ_{m-2} is shown in Fig. 7 as a function of q_-^1 at constant values of q_m. The relationship shown in Fig. 7 indicates a linear function of q_-^1 and the slopes of these straight lines are almost the same except at very negatives of q_m. This slope has the relationship with the standard free energy of adsorption, ΔG:[28-30]

$$\left(\frac{\partial\phi_{m-2}}{\partial q_-^1}\right)_{q_m} = \frac{RT}{F}\left(\frac{\partial(-\Delta G/RT)}{\partial q_m}\right)_{T,P} \tag{14}$$

Therefore, if we base our discussion on Eq. (14), we may infer that the free energy of adsorption is a linear fuction of q_m and is independent of q_-^1. This behaviour has been shown in the aqueous solution of ions with high specific adsorptivity ions such as I^-[17] and Cl^-[7] in the DMSO solution.[7] However, Eq. (14) is only an approximation because it does not take into account the contribution of the diffuse double layer. This contribution may be very small in the potential range where the specific adsorption of ions is predominant. On the other hand, it becomes effective in other potential ranges. This is supported by the results that the deviation from the constant slope in Fig. 7 increases with the decrease in q_m (*i.e.*, becoming more negative).

The potential of ϕ_{m-2} can be divided into two components according to the following equation:[31]

$$d\phi_{m-2} = \left(\frac{\partial\phi_{m-2}}{\partial q_-^1}\right)_{q_m} dq_-^1 + \left(\frac{\partial\phi_{m-2}}{\partial q_m}\right)_{q_-^1} dq_m. \tag{15}$$

In Eq. (15), we define the corresponding integral capacities, ${}_{q_-^1}C^i$ and ${}_{q_m}C^i$, according to Grahame and Parsons by:[32]

$$\begin{aligned} {}_{q_-^1}C^i &= 1/(\partial\phi_{m-2}/\partial q_-^1)_{q_m} \\ {}_{q_m}C^i &= 1/(\partial\phi_{m-2}/\partial q_m)_{q_-^1} \end{aligned} \tag{16}$$

As a first approximation, we assumed that the inner layer can be represented by two condensers in series,

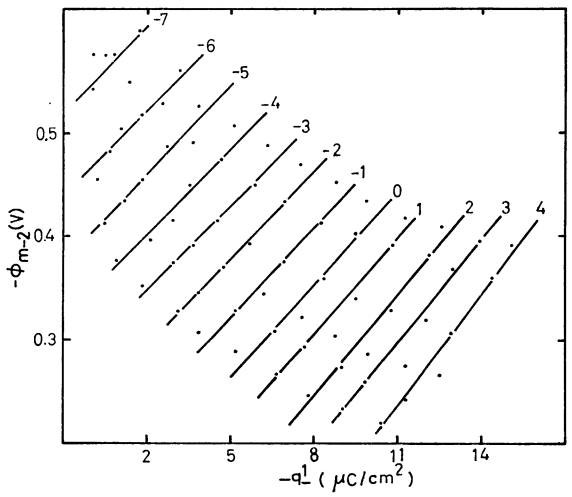

Fig. 7. Potential difference across the inner layer generated by specifically adsorbed anion (ϕ_{m-2}), as a function of the charge due to specifically adsorbed bromide ions (q_-^1) at the constant electrode charge. The value of electrode charge is indicated by each line in $\mu C/cm^2$.

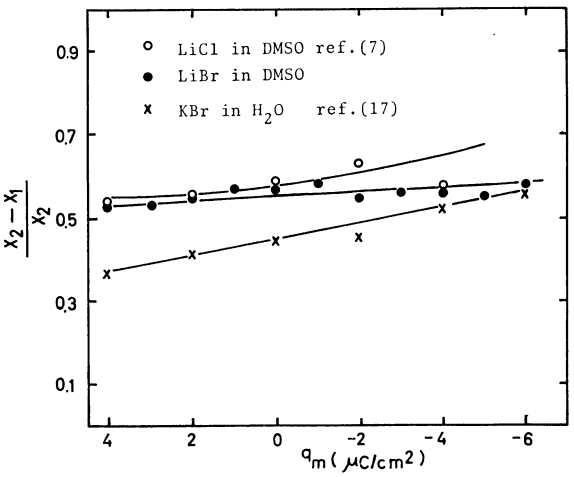

Fig. 8. Variation of distance ratio ($(x_2-x_1)/x_2$) as a function of the electrode charge and comparison it with other data.

the mercuy surface to the inner Helmholtz plane (iHp) and the iHp to the oHp; furthermore, we assumed that the dielectric constants are equal in these two layers. Then we computed the distance ratio $(x_2-x_1)/x_2$ from this relationship:

$$\frac{x_2-x_1}{x_2}=\frac{{}_{q_m}C^i}{{}_{q^-}C^i}, \tag{17}$$

where x_1 and x_2 are the distances from the metal surface to the iHp and to the oHp respectively. From the results of Fig. 7 we found the integral capacities to be ${}_{q^-}C^i=30\sim36$ μF/cm² and ${}_{q_m}C^i=16\sim21$ μF/cm². These values are comparable to those for LiCl in DMSO. The distance ratios mentioned above found to be 0.52—0.58; the dependence of this ratio on q_m is shown in Fig. 8, where it is also compared with other electrolytes and aqueous system. The plot in the present study seems to be constant over the range of q_m studied and does not show a definite tendency to increase with a decrease in the q_m values. The values of the distance ratio are greater than the corresponding values of bromide ions in an aqueous system[17] (0.35—0.55) in the range of $q_m>0$. However, they are nearly the same at negative values of q_m. If we assume x_2 to be the sum of the thickness of DMSO monolayer (4.8 Å)[33] and the crystallographic radius of the lithium ion of 0.68 Å,[34] the resulting value of x_1 (*i.e.*, the thickness of the iHp) varies from 2.3 Å to 2.6 Å. These are greater than the crystallographic radius of the bromide ion (1.96 Å).[34] If x_1 is assumed to be 1.96 Å, the thickness of the oHp becomes from 4.1 to 4.7 Å. Considering the incompliteness of the solvent monolayer formation, we may say that some of the lithium ions sit inside the DMSO monolayer and that others are present on the outside of the monolayer of solvent molecules. However, this discussion has been based on a simple condenser model; it is only a qualitative discussion. For more detailed discussion, it will be necessary for us to take into consideration the dependence of the dielectric constant on the distance from electrode surface, the influence of the variation in solvent dipoles, and so on.

The authors with to thank Miss Masako Arai and Mr. Masami Iiyama who assisted them extensively in this study.

References

1) J. N. Butler, *J. Electroanal. Chem.*, **14**, 89 (1967).
2) R. Jasinski, "High Energy Batteries," Plenum Press, New York (1967).
3) J. N. Butler," Advances in Electrochemistry and Electrochemical Engineering," Vol. 7, Wiley-Interscience, New York (1970), p. 77.
4) B. Burrows, *J. Electrochem. Soc.*, **118**, 1130 (1971).
5) I. M. Kolthoff and T. B. Reddy, *ibid.*, **108**, 980 (1961).
6) R. Payne, *J. Amer. Chem. Soc.*, **89**, 489 (1967).
7) S. H. Kim, T. N. Andersen, and H. Eyring, *J. Phys. Chem.* **74**, 4555 (1970).
8) G. J. Hills and R. M. Reeves, *J. Electroanal. Chem.*, **41**, 213 (1973).
9) R. S. Hansen, D. J. Kelsh, and D. H. Grantham, *J. Phys. Chem.*, **67**, 2316 (1963).
10) D. E. Broadhead, R. S. Hansen, and G. W. Jr. Potter, *J. Colloid Interface Sci.*, **31**, 61 (1969).
11) Y. Inoue and K. Niki, *Rev. Polarography* (Kyoto), **18**, 49 (1972).
12) M. Salomon, *J. Electrochem. Soc.*, **116**, 1392 (1969).
13) J. S. Dunnett and R. P. H. Gasser, *Trans. Faraday Soc.*, **61**, 922 (1965).
14) K. Yamamoto, unpublished data.
15) R. Parsons, *Trans. Faraday Soc.*, **64**, 1638 (1968).
16) M. A. V. Devanathan and B. V. K. S. R. A. Tilak, *Chem. Rev.*, **65**, 635 (1965).
17) J. Lawrence and R. Parsons, *J. Electroanal. Chem.*, **16**, 193 (1968).
18) D. C. Grahame and B. Sorderberg, *J. Chem. Phys.*, **22**, 449 (1954).
19) R. A. Hovermale and P. G. Sears, *J. Phys. Chem.*, **60**, 1579 (1956).
20) P. Delahay, "Double Layer and Electrode Kinetics," Wiley, New York, 1965.
21) R. Payne, *J. Electroanal. Chem.*, **7**, 343 (1964).
22) R. Payne, *J. Chem. Phys.*, **42**, 3371 (1965).
23) R. Parsons, Proc. Intern. Congr. Surface Activity, 2nd, London, 3, 38 (1957).
24) D. M. Mohilner, "Electroanalytical Chemistry," Vol. 1, Mercel Dekker, New York (1966), p. 291.
25) G. J. Hills and R. M. Reeves, *J. Electroanal. Chem.*, **38**, 1 (1972).
26) A. J. Parker, *Quart. Rev.* (London), **16**, 163 (1962).
27) M. Salomon, *J. Electrochem. Soc.*, **117**, 325 (1970).
28) R. Parsons, *Trans. Faraday Soc.*, **55**, 999 (1959).
29) J. M. Parry and R. Parsons, *ibid.*, **59**, 241 (1961).
30) J. Lawrence and R. Parsons, *ibid.*, **64**, 751 (1968).
31) R. Parsons, "Advance in Electrochemistry and Electrochemical Engineering," Vol. 1, 1, Willey-Interscience, New York (1961).
32) D. C. Grahame and R. Parsons, *J. Amer. Chem. Soc.*, **83**, 1291 (1961).
33) R. Thomas, C. R. Shoemaker, and K. Eriks, *Acta Crystallogr.*, **21**, 12 (1966).
34) R. C. Weast, Ed., "Handbook of Chemistry and Physics," 50th ed. The Chemical Rubber Publishing Co., Cleveland, Ohio (1969).